Spectroscopy of the BL Lac H1426+428 with the XMM RGS

I. Sakelliou, G.Branduardi-Raymont, T. Harries, J. Rainger
Mullard Space Science Laboratory, UCL, UK

S. Kahn, M. Sako
Columbia Astrophysics Laboratory, USA

J. Kaastra, F. Paerels
Space Research Organization of the Netherlands

D. Liedahl
Lawrence Livermore National Laboratory, USA

ABSTRACT

The Reflection Grating Spectrometer (RGS) on XMM, with its high resolving power and collecting area, will open brand new opportunities for X-ray astronomy, producing X-ray spectra of a similar quality to that of optical spectroscopy: for example, for the brightest objects we expect that it will be possible to measure individual lines parameters and line ratios directly from the observed spectra without resorting to a traditional chi-square comparison of model spectra with observations.

This poster presents RGS simulations of the spectra of the BL Lac object H1426+428. The results are obtained using the ESA's SCISIM package, which mimics the performance of each component in the RGS instrument chain. Indications of how RGS data may be analyzed are also given.

It is shown that a 50 ksec exposure with the RGS will resolve the shape of the absorption feature so far just detected in the spectrum of H1426+428, and help us to accurately calculate its depth and width, and determine the energy at which the absorption happens.

1. Introduction

The BL Lac object H1426+428 was observed with the BBXRT with moderate energy resolution (∼90 eV at 1 keV). This data set provided evidence for the presence of an absorption feature at ∼0.6 keV (Sambruna et al. 1997). Unfortunately, the quality of the data was not good enough to confidently constrain the shape and parameters (such as the depth and width) of the absorption feature. The knowledge of these quantities is vital if we are to understand what causes the absorption and the nature of the absorber.

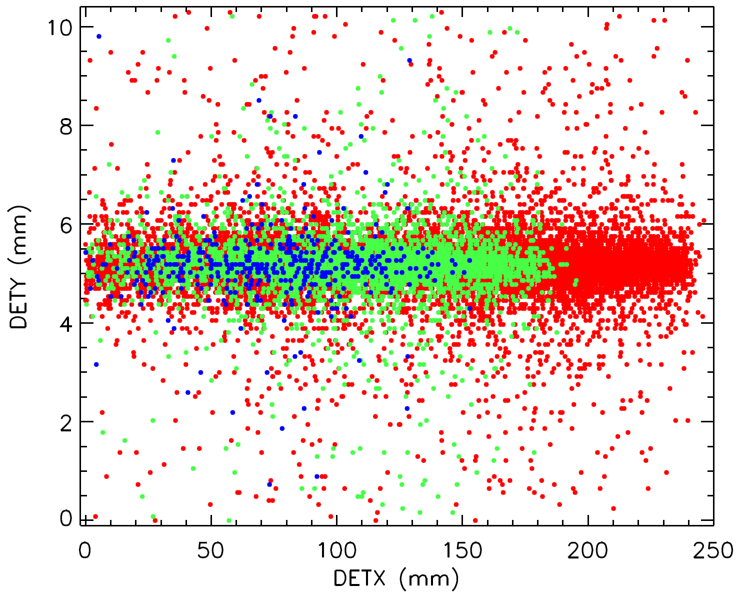

Fig. 1.— A scatter plot of the SCISIM output for model A. It shows the position of the dispersed photons in all nine RGS CCDs. The separate but overlapping orders are shown with different colors: first order = red, second order = green, third order = blue.

H1426+428 will be observed for 50 ksec as part of the XMM RGS Guaranteed Time programme. Here we present the expected results from the RGS. The simulations were performed with ESA's SCISIM (v.2.0.2) package.

2. Simulated Spectral Models

The best fit model parameters derived from the spectral analysis of the BBXRT data (Sambruna et al. 1997) were used as input for the simulations. The two trial spectral models which are compared are:

1. **model A**: a broken power law ($E_0 = 0.79$ keV, $\Gamma_1 = 1.41$ below E_0, $\Gamma_2 = 2.20$ above E_0) with an absorption edge ($E = 0.576$ keV, $\tau = 1.075$)
2. **model B**: a broken power law ($E_0 = 2.09$ keV, $\Gamma_1 = 1.84$, $\Gamma_2 = 2.29$) with an absorption notch [$E = 0.668$ keV, $f_c = 1(>0.3)$, and width ΔE=0.057 keV]

For both cases the absorption due to the Galactic $N_{\rm H}$ (=1.41×10^{20} cm^{-2}) was included, and the exposure time was set to 50 ksec.

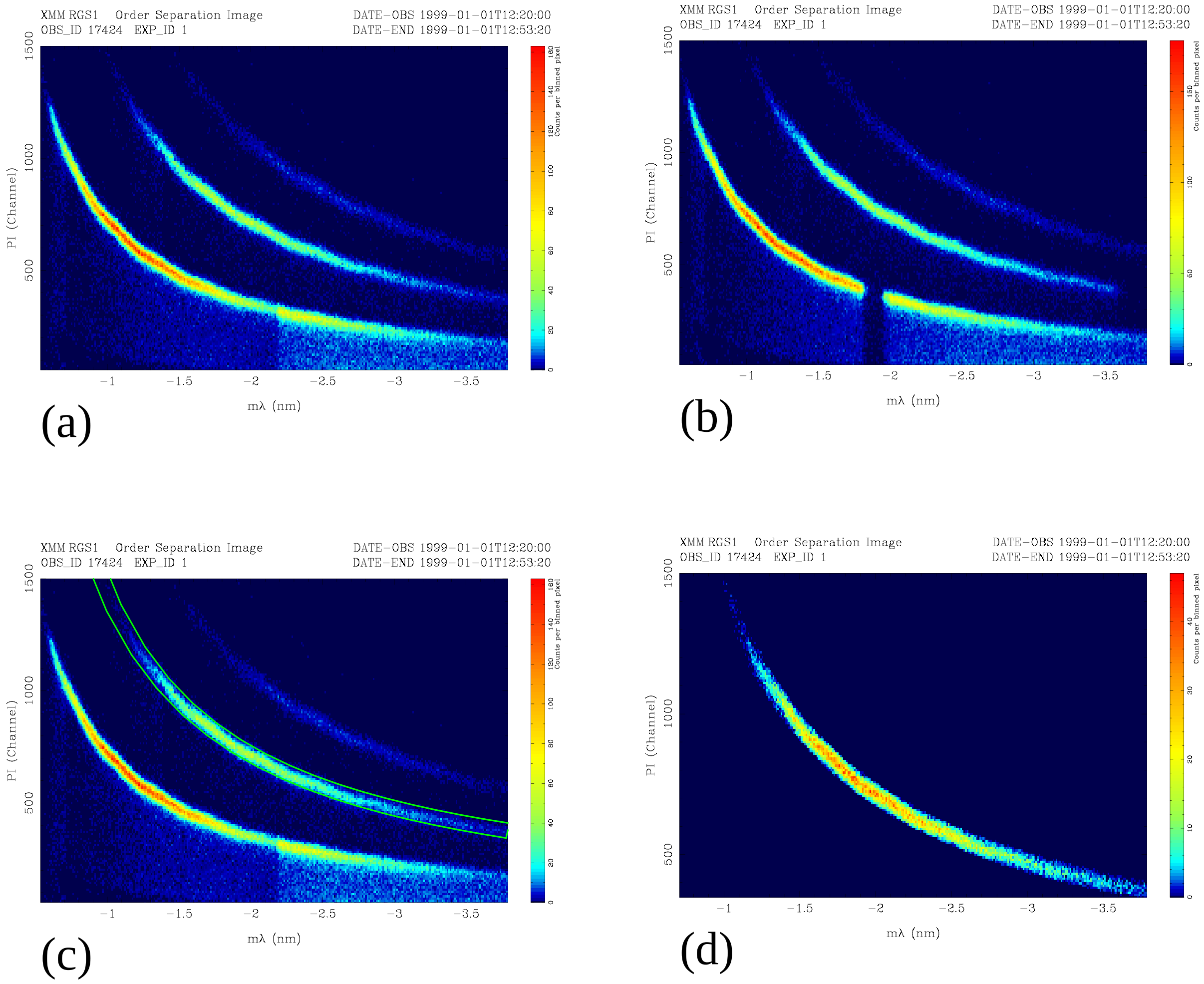

Fig. 2.— Banana-plots for the two different SCISIM simulations. In the first three plots the first order is the brightest banana, and the third order is the faintest. (a) Banana-plot for spectral model A, in which the absorption feature is an edge at ∼2.2 nm (E=0.576 keV). (b) Banana-plot for model B. In this case the absorption feature is a notch at ∼1.9 nm (E=0.668 keV) with $f_c = 1$, and width ΔE=0.057 keV, appearing as a gap in the first order. (c) The same as (a). The green line is the mask used to separate the second order. (d) The extracted second order for model A.

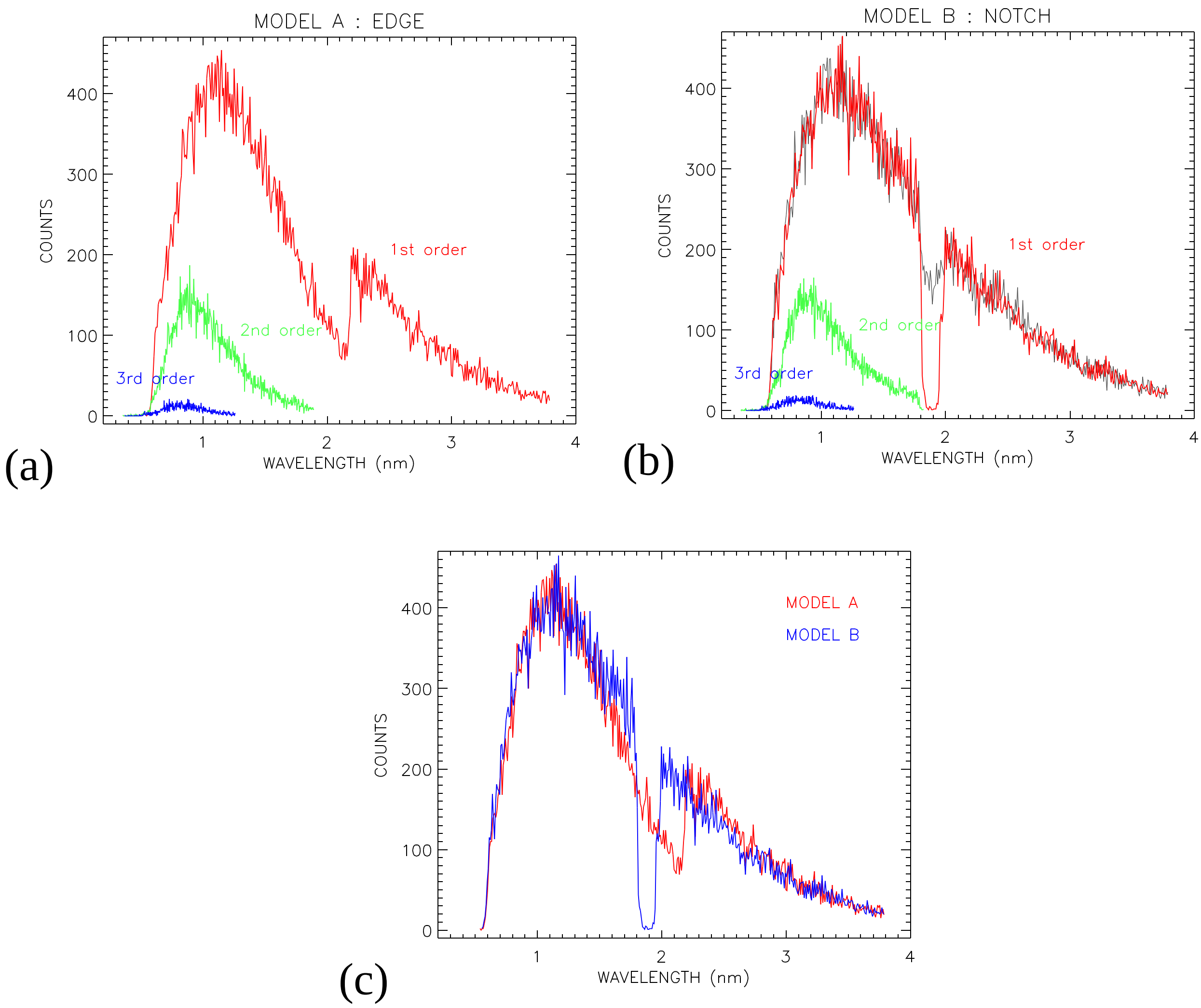

Fig. 3.— Predicted spectra of the BL Lac H1426+428 for the two trial spectral models: (a) model A, and (b) model B (see text). The three different orders for each model are also presented. The thin black line in (b) is the result for a shallower notch with f_c=0.3. In (c) the first orders of the two models are compared.

3. RGS Data Analysis

In Fig. 1. the position of the dispersed photons in the plane of the RGS Focal Camera CCDs is plotted. Such a plot cannot be used directly to extract information about the spectrum of a source, since photons with the same $m\lambda$ (where m is the spectral order e.g. -1, -2, and λ the wavelength) lie at the same position on the x-axis in Fig. 1. This problem can be overcome and the different orders are finally separated by using the intrinsic energy resolution (pulse height information) of the CCDs. By plotting the CCD's pulse invariant (PI, i.e. the pulse height corrected for CCD gain) versus the distance along the dispersion direction (DETX) the different orders become well distinguishable. Figure 2. presents what are often called 'banana'-plots: it is easily seen that the photons from each order appear in a well defined region, a 'banana'. Additionally, in Fig. 2. the detector's coordinate DETX has been translated into wavelength $m\lambda$ by using the grating dispersion equation (Brinkman et al. 1996).

Using a banana-plot, orders are separated by defining a region which includes only the desired order. For example, in Fig. 2.(c) the green line shows such a mask, used to extract $\sim$90% of the second order's photons. The separated second order is shown in Fig. 2.(d). Finally, the projection of Fig. 2.(d) onto the wavelength axis provides the spectrum (Fig. 3.).

4. Results

The extracted spectra for the two models, computed in bins of 0.085 nm for the first order, 0.04 nm for the second, and 0.02 nm for the third are shown in Fig. 3. The absorption feature lies in the wavelength range covered only by the first orders in both spectral models. For this reason only the first orders are compared in Fig. 3(c).

Figure 3.(c) shows clearly that a 50 ksec observation of the BL Lac 1H1426+428 with the XMM RGS will enable us to accurately determine the properties of its spectrum, and subsequently to answer questions concerning the nature of the absorber and the physical processes which take place withing its host galaxy.

REFERENCES

Sambruna R. M., George I. M., Madejski G., Urri C. M., Turner T. J., Weaver K. A., Marashi L., Treves A., 1997, ApJ, 483, 774

Brinkman A. C., Aarts H. J. M., den Boggende A. J. F., Bootsma T., Dubbeldam L., den Herder J. W., Kaastra J. S., de Korte P. A. J., van Leeuwen B. J., Mewe R., van Zwet E., Decker T., Hailey C. J., Kahn S. M., Paerels F., Pratuch S., Rasmussen A., Branduardi-Raymont G., Guttridge P., Bixler J., Thomsen K., Zehnder A., Erd C., 1996, SPIE, 2808, 463